Solar Energy Materials & Solar Cells 245 (2022) 111877

Contents lists available at ScienceDirect

Solar Energy Materials and Solar Cells

journal homepage: www.elsevier.com/locate/solmat

A new configuration of V-trough concentrator for achieving improved concentration ratio of >3.0x

Mohammad Alnajideen [a,b], Min Gao [a,*]

[a] School of Engineering, Cardiff University, Cardiff, CF24 3AA, Wales, UK
[b] Faculty of Engineering, Mutah University, Al-Karak, 61710, Jordan

ARTICLE INFO

Keywords:
Concentrator photovoltaic
V-trough concentrator
Optical efficiency
Angular response
CPV system

ABSTRACT

A new configuration of V-trough solar concentrator is proposed, constructed and investigated in an attempt to improve the concentration ratio of the V-trough concentrators. The new design consists of two conventional V-trough concentrators arranged in a cross, which lead to improvement in concentration ratio and angular response. The results of an experimental study show that the concentration ratio of this new configuration (referred to as OVSC) is 40%–60% higher than its corresponding conventional V-trough solar concentrator (CVSC) with additional benefits. The study reveals that the angular response of this new configuration is better than conventional V-tough concentrator with a potential to reduce the cost of concentrators by using less reflector materials. Surprisingly, the improvement in the concentration ratio is not accompanied by significant reduction in optical efficiency and light uniformity, making it a better alternative for low-cost and low concentration applications in future.

1. Introduction

Solar concentrators have been widely studied since 1970s [1–10]. Concentrator Photovoltaic (CPV) is an alternative system to the flat-plate PV module to produce electricity at affordable and competitive prices. CPV systems use lenses or mirrors to concentrate the sunlight onto a small area of PV cells in order to use less PV materials, increase the system efficiency, generate more electrical power, and thereby reduce their cost and maintenance [11,12]. Developing high-performance concentrators is part of important efforts for achieving economically viable PV systems [13–15]. Although significant reduction in the price of silicon solar cells in recent years has made CPV approach no longer attractive for silicon panels, the concentrator may still play a role in improving the economic viability of more expensive solar cells, such as GaAs and InP cells, or thermal system.

V-trough Solar Concentrator (VSC) and Compound Parabolic Concentrator (CPC) are non-imaging CPV systems and they have been employed as primary or secondary optical element (SOE) [16,17]. In recent years, efforts have been reported to investigate CPV systems for building-integrated applications [18–20]. One of the research focuses is to improve the performance of the CPC [21–28], including a focus on the optical efficiency, acceptance angle and light uniformity across the PV cell [21–24,28]. The CPC appears to be a preferred choice over VSC because its compactness and higher concentration ratio [29,30]. The drawback of VSC compared to CPC is the difficulty to obtain the concentration ratio that is higher than 3x [31,32]. Nevertheless, the VSC has the advantages of (i) the uniform illumination on the absorber area that is desirable for PV applications, (ii) simple and easy to design and fabricate due to the flat reflector, and (iii) low cost due to the simplicity in the structure and fabrication [33–35].

Since the proposal of VSC by Hollands [36] in 1971, many works have been reported focusing on analysis of its optical performance and the potential for energy collection in a particular location over a period with or without tracking [37–45]. Experimental works were also conducted to evaluate the optical performance of the VSCs. Fig. 1 shows a collection of the experimental works reported over the past 50 years [46–51]. The VSCs were all designed with a reflector tilt angle at 60°. The highest concentration ratio obtained experimentally is 1.98x by Wang et al. [33] and the highest optical efficiency is 89.9% reported by Singh et al. [35]. To our knowledge, no work has been reported to show that a concentration ratio of >3.0x can be obtained in V-trough solar concentrators. In this work, we report a new configuration of VSC design that enables higher concentration ratio while maintaining good optical efficiency and angular response. The new design consists of two

* Corresponding author.
E-mail address: Min@Cardiff.ac.uk (M. Gao).

https://doi.org/10.1016/j.solmat.2022.111877
Received 23 September 2021; Received in revised form 12 June 2022; Accepted 26 June 2022
Available online 8 July 2022

conventional V-trough concentrators arranged in cross shape. A systematic investigation was performed to evaluate the characteristics of this new design, which include the concentration ratio, optical efficiency, angular response, light uniformity, and the cost of production. To demonstrate the advantages and unique characteristics of this new design, the study was performed in comparison with conventional VSCs.

2. Design parameters for VSC

The basic structure of a conventional VSC consists of two symmetrical flat reflectors forming a "V" shape with a PV cell at the bottom part as shown Fig. 2. The reflectors concentrate the incoming solar radiation on to the absorber area, where a PV cell or thermal receiver is positioned. A key advantage of VSC is the simplicity in its design and construction. A proper design involves determine the tilt angle, φ, and reflectors length, L, based on a well-established theory [36]. The geometrical concentration ratio, CR_{geo}, of a VSC is defined as the ratio of the aperture area, A, to the absorber area, a,

$$CR_{geo} = \frac{A}{a} = \frac{W_{ap}}{W_{ab}} \tag{1}$$

where, W_{ap} and W_{ab} are the width of the aperture and the absorber, respectively. In the case of the normal light incident (i.e., the angle of light incidence $\alpha = 0°$) and assuming that the number of light reflections is $N = 1$, the geometrical concentration ratio, CR_{geo}, can be expressed in terms of vertex angle, Ψ [36],

$$CR_{geo} = 1 + 2\rho cos\Psi \tag{2}$$

where, ρ is the reflectivity of the reflector surface. Ψ is related to the side wall length, L, the width of the absorber, W_{ab}, and the trough angle, θ, by [36].

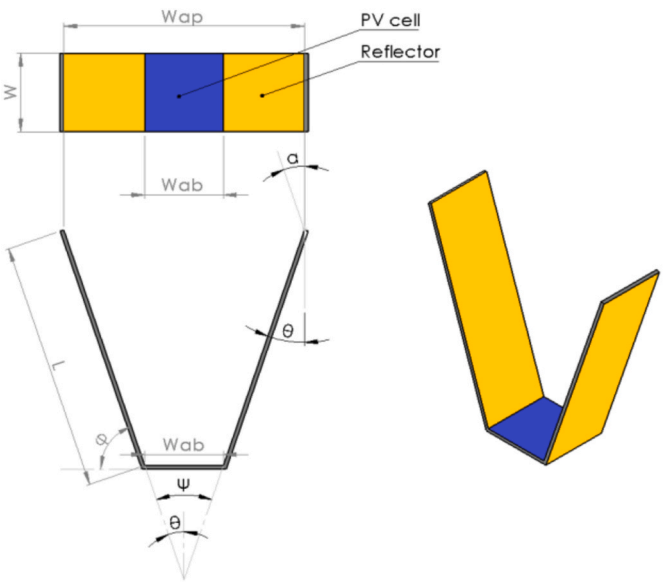

Fig. 2. Schematic diagram of V-trough solar concentrator.

$$(L / W_{ab}) = \frac{\cos\Psi}{\sin\theta} \tag{3}$$

Equation (2) indicates that the concentration ratio of VSC is limited to 3x for $N = 1$. This assumption is usually valid when Ψ is large. When Ψ is very small, the light may undergo multiple reflections before reaching the absorber area. In such case, the number of the light reflections is $N \geq 1$ and the CR_{geo} is given by [36].

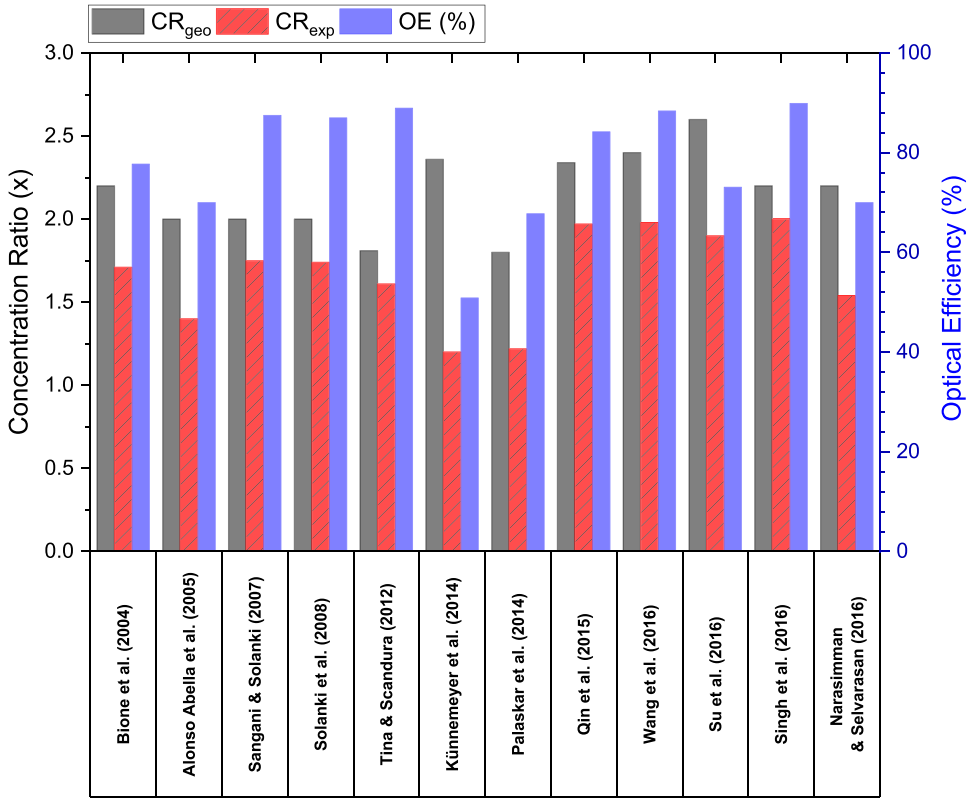

Fig. 1. Experimental results of the concentration ratio and optical efficiency of VSCs reported in recent years. CR_{geo} and CR_{exp} are the geometrical and experimental concentration ratio, respectively and OE is the optical efficiency of the concentrators.

$$CR_{geo} \geq 1 + \frac{2\sin(N\theta)\cos[(N+1)\theta]}{\sin\theta} = \frac{\sin[(2N+1)\theta+\alpha]}{\sin(\theta+\alpha)} \quad (4)$$

The trough angle, θ, is limited by [38,41].

$$\frac{90-\alpha}{2N} \geq \theta \geq \frac{90+\alpha}{2(N+1)} \quad (5)$$

Equation (3) in this case can be expressed as [38,41].

$$(L/W_{ab}) = \frac{\sin[(2N+1)\theta+\alpha] - \sin(\theta+\alpha)}{2\sin(\theta+\alpha)\sin\theta} \quad (6)$$

The optical efficiency, *OE*, of a practical concentrator is defined as [52–54].

$$OE = \frac{CR_{eff}}{CR_{geo}} \quad (7)$$

where, CR_{eff} is the actual concentration ratio determined from the experiment. In a perfect case, CR_{eff} is equal to the geometrical concentration ratio. In practice, it is smaller than the geometrical concentration ratio due to various losses. CR_{eff} can be calculated from the short-circuit current (I_{sc}) of a PV cell under concentration divided by the corresponding short-circuit current without concentration (i.e., the bare cell).

The light uniformity, $\overline{U}$, of a concentrator is a measure of uniform light distribution in terms of the intensity over the absorber area. It can be evaluated using [52–54],

$$\overline{U} = 1 - \frac{I_{max} - I_{min}}{I_{max} + I_{min}} \quad (8)$$

where, I_{max} and I_{min} are the maximum and the minimum irradiances detected over the absorber area.

3. Experimental

3.1. Concentrator design

Four conventional VSCs (CVSC) of different concentration ratios were designed as the benchmarks for this study. The theory described in section 2 was employed to determine the geometrical concentration ratio, CR_{geo} and the aspect ratio (L/W_{ab}) of concentrators for a given φ. To simplify the design procedure, this study focuses on the cases of operating under normal irradiance of light (i.e., $\alpha = 0°$) [52]. Since the PV cell to be used in this study has a dimension of 10 mm × 10 mm, the width of the absorber of the VSCs was fixed to 10 mm (i.e., $W_{ab} = 10$ mm). The appropriate *N* value was determined using Equation (5). In addition, the design needs to consider the restriction of the testing system used in this study. The aperture area of the concentrator must be smaller than the illumination area of the solar simulator. The height of the VSC must be shorter than the distance between the solar simulator and testing stage. Table 1 presents the design parameters for four CVSCs selected for fabrication. Among them, the concentrator with $\varphi = 60°$ is a widely employed design in many published works. The other three angles are selected to increase the concentration ratio, CR_{geo}.

An initial attempt to increase the concentration ratio of the V-trough concentrators was to follow the configuration of cross compound parabolic concentrator (CCPC) but using the flat reflectors. This led to a pyramid configuration, which is thereafter referred to as the Pyramid VSC (PVSC) as shown in Fig. 3a–I. The design parameters for four corresponding PVSCs are also listed in Table 1. Unlike the CVSCs, where the calculated CR_{geo} agrees roughly with the actual measured concentration ratio, CR_{eff}, the actual concentration ratios of the PVSCs are significantly lower than the calculated values.

Simulation using raytracing software (TracePro) was performed to identify the cause for such significant difference between the calculated and measured concentration ratios in the PVSCs. The results of simulation (Fig. 3a–II) shows clearly that a significant part of the incident light is reflected out of the PVSC, rather than concentrated onto the absorber area. The simulation is supported by the experimental observation of the reflected light escaped from the concentrator shining on the wall of the Faraday cage as shown in Fig. 3b. A detailed inspection of the simulation results reveals that the corner areas (i.e., the black area in Fig. 3a–III) in the PVSC do not contribute to light concentration to the absorber area. The experimental work using light shutters confirms this finding and explains a significant discrepancy between the calculated CR_{geo} (9.36x) and the measured CR_{eff} (4.70x) for PVSCs. Clearly, these corner areas do not contribute to the light concentration but consume more reflective materials and resulted in poor optical efficiency of the PVSCs, which is significantly lower than that of the CVSCs, as illustrated in Table 2.

A solution to improve the optical efficiency of the PVSCs is to eliminate the "inactive" reflective areas in the PVSCs. This led to a new configuration of V-trough concentrators as shown in Fig. 4. The new design (Fig. 4a) consists of two V-troughs (golden colour areas) arranged in a cross-shape with a common PV cell area in the centre (blue colour area). It has the appearance of the Onagraceae flower (Fig. 4b) and thereafter is referred to as the Onagraceae V-trough Solar Concentrator (OVSC). The CR_{geo} of the OVSC can be determined using the following equations, which are simple modifications of Equations (1) and (4),

$$CR_{geo} = \frac{A}{a} = \frac{2W_{ap} - W_{ab}}{W_{ab}} \quad (9)$$

$$CR_{geo} \geq 1 + \frac{4\sin(N\theta)\cos[(N+1)\theta]}{\sin\theta} \quad (10)$$

An OVSC uses half of the reflective materials of its corresponding PVSC to achieve the same concentration ratio, which is higher than that of its conventional VSC counterpart. In addition, a gapless panel can also be formed by arranging the OVSCs in a pattern as shown in Fig. 5, even though it seems to be difficult at first glance. In order to evaluate their optical performance, four OVSCs were designed, which have the same tilt angles and aspect ratios to their corresponding CVSC benchmarks. Table 3 summarises the design parameters and the resultant geometrical concentration ratios of four CVSCs and OVSCs designed for experimental investigation.

Table 1
Geometrical and experimental concentration ratios of conventional and pyramid VSCs.

VSC	$\Psi = (2\theta)$	φ	(L/W_{ab})	N	CR_{geo}		$CR_{eff} \pm 0.01$	
					CVSC	PVSC	CVSC	PVSC
VSC-I	60°	60°	1.00	1	2.00	4.00	1.76	2.47
VSC-II	50	65°	1.52	1	2.29	5.22	2.07	3.17
VSC-III	44	68°	2.01	2	2.51	6.29	2.33	3.68
VSC-IV	38	71°	3.16	2	3.06	9.36	2.87	4.70

3.2. Fabrication of concentrators

The frames of concentrators were designed using Solidworks® software and printed using a Fused Deposition Modelling (FDM) 3D printer (ULTIMAKER Extended 2+), which provides accurate and high surface finish and robust structures. A black PLA filament (1.24 g/cm^3 and 2.85 mm diameter) was used to construct the frames of concentrators with a high-temperature resistance (160 °C), resolution of 0.02 mm and for a cost of \$0.01/cm^3. The dimensions of the printed frames were measured using a Quick-Vision Microscope (PJ-A3000 Profile Projector, Mitutoyo Inst.) to ensure that the dimensions are in good agreement with the original CAD design within a small tolerance of ±0.1 mm.

Four specular thin-film reflectors (MIRO-SUN, MIRO, Vega and 3 M Tape) were tested using a spectroradiometer and their reflectance are shown in Fig. 6a. It can be seen that the aluminium thin-film reflector (MIRO-SUN) has the highest spectral reflectivity (95%) among all tested reflectors. It also has high reflectance at high angles of light incidence

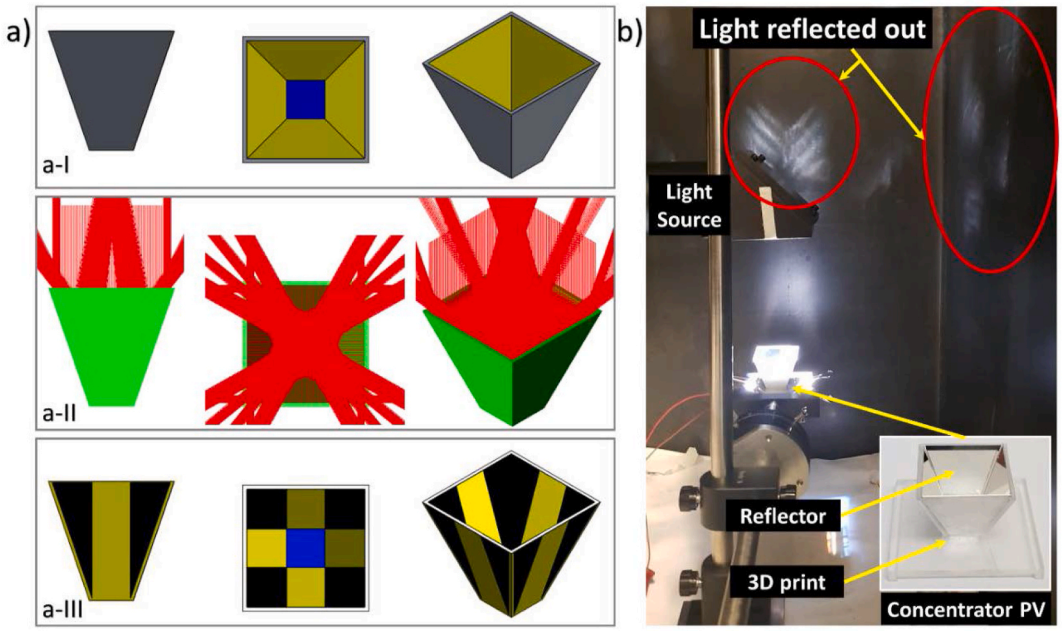

Fig. 3. (a) PVSC design, raytracing and active and inactive area, respectively and b) a photograph of the PVSC under the light beam.

Table 2
Optical efficiency and the surface area of the conventional and pyramid VSCs.

VSC	Optical Efficiency, *OE* (%) ± *0.01*		Area of Reflectors (mm^2)	
	CVSC	PVSC	CVSC	PVSC
VSC-I	88.18	61.74	200	600
VSC-II	90.44	60.72	304	1000
VSC-III	93.02	58.51	403	1413
VSC-IV	93.79	50.20	633	2569

(AOI) that are preferred in the concentrator design (Fig. 6b). Consequently, MIRO-SUN film was chosen for this study. This reflective material is anodized aluminium film, which has water-resistant coating and specially designed for solar concentrators. The dimensions of the reflectors were drawn using Solidworks® and cut using CNC machine (LPKF Laser Machine) to ensure precision. The thickness of the reflector films (0.20 mm) was taken into consideration in the design. The reflector films were glued on inner surfaces of the printed VSC frames. Fig. 7 shows the photograph of the fabricated CVSCs and OVSCs used in this study.

3.3. Experimental setup and testing procedures

To characterise the optical performance of the fabricated concentrators, a VSC-PV assembly was constructed. A Laser Grooved Buried Contact (LGBC) monocrystalline silicon PV cell (10 mm × 10 mm) was mounted on a Direct Copper Bonded (DCB) alumina substrate, which is electrically insulating and thermally conducting. The DCB substrates were made based on customised design. The substrate has a tin-coated copper layer on the top for soldering the front and rear contacts of the PV cell. Low-temperature solder was used to prevent the cell damage and increase in the series resistance. The VSC-PV assembly was mounted on an aluminium water-cooled stage to maintain the temperature of the PV cell at 25 °C during the test, which can rotate between 0° and 180° at a step of 5°. This stage was developed for angular response measurements by Al-Shidhani et al. [53]. A type K thermocouple was placed in the vicinity of the top surface of the PV cell and another is insisted in a groove between the ceramic plate and the water-cooled stage. All gaps between interfaces are filled with the heat sink compound (thermal conductivity of 2.9 W/m.K, RS217-3835) to ensure good thermal contact. Fig. 8 shows the schematic diagram of the constructed VSC-PV assembly mounted on the rotary stage. In this design, the VSC can be removed and replaced without affecting other parts, enabling comparative study under the identical condition except for different VSCs.

The testing setup for evaluation of the fabricated concentrators is

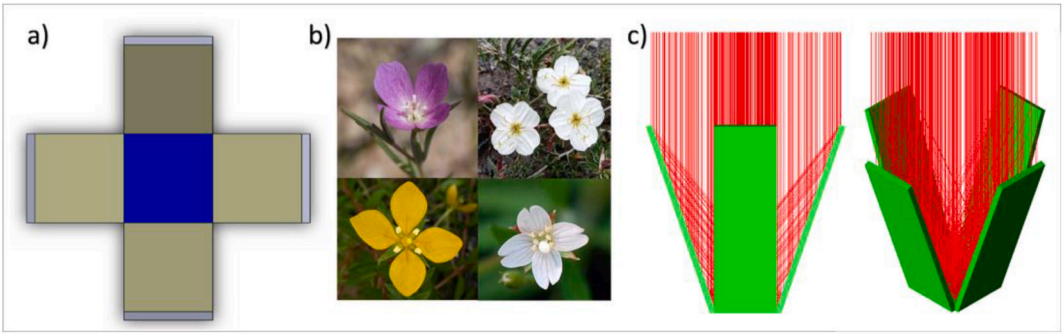

Fig. 4. Schematic diagrams of a new configuration of V-trough concentrator (a) OVSC design, (b) Onagraceae flowers and c) images of raytracing results for the OVSC.

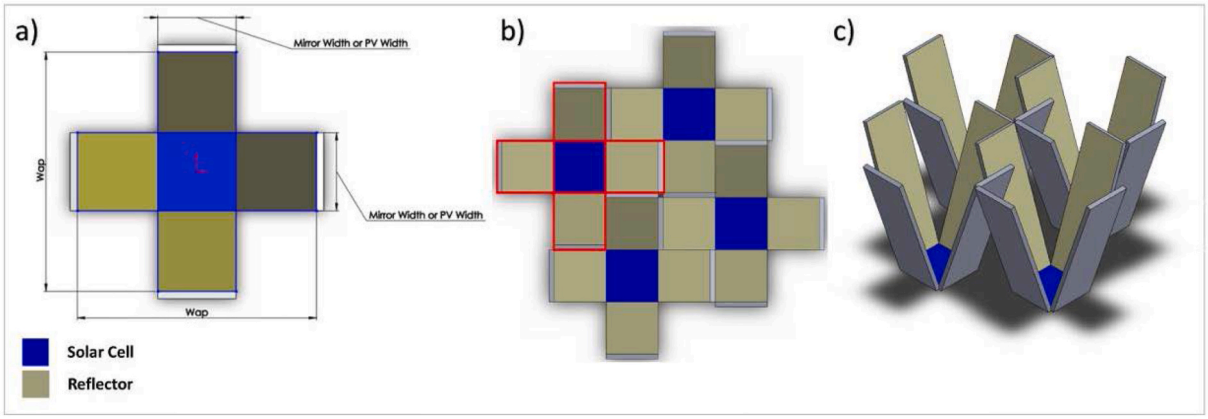

Fig. 5. Schematic of an Onagraceae concentrator panel (a) Single OVSC (b) top view of OVSC panel, and (c) isometric view of OVSC panel.

Table 3
The design parameters and the resultant geometrical concentration ratios of conventional VSCs and Onagraceae VSCs.

VSC	φ	(L/W_{ab})	N	CR_{geo}		
				CVSC		OVSC
I	60°	1.00	1	2.00		3.00
II	65°	1.52	1		2.29	3.57
III	68°	2.01	2	2.51		4.02
IV	71°	3.16	2	3.06		5.12

shown in Fig. 9. The experiments were carried out under a uniform illumination of a class ABB solar simulator (Orial LCS-100, Newport instrument). Both VSC-PV assembly and solar simulator are placed inside a Faraday-cage and the tests were performed at the standard test condition (1000 W/m^2, AM1.5G, 25 °C) and repeated for at least three times. The block on the left side of Fig. 9 is used for measuring I–V curves of the PV cells under illumination using AUTOLAB I–V tracer (PGSTAT302 N). All tests were repeated at least 3 times and the data presented is the average value of 3 measurements. The block on the right side is used for measuring the spectral response and the light uniformity using a spectroradiometer (StellerNet instrument) covering light spectrum of 300 nm–1700nm. During the test, the temperatures of the PV cell and ambient were monitored and recorded using type K thermocouples connected to a computer via a PICO data logger. The temperature of the PV cell was controlled by a water circulating bath (Thermo-HAAKE-B3).

Two techniques were employed in this study to determine the concentrator ratio. The first one is based on the I–V curves of the PV cell acquired using the AUTOLAB. The concentration ratio is calculated from the I_{sc} of the PV cell with a concentrator divided by that without the concentrator (i.e., bare cell). The second one is determined in a similar way by using the light intensities measured using the spectroradiometer. Simulation was also performed to determine the concentration ratio of the concentrators, assuming that the reflectivity of the reflectors was 95%. This assumption has been chosen to meet the reflectance of the candidate reflector measured in this study, see section 3.2.

The light uniformity on the absorber surface of the concentrators was investigated using the spectroradiometer. The absorber area was divided into nine equal areas of 1.5 mm^2 each in a windowpane pattern. The light sensor of the spectroradiometer was positioned in the centre of each division for light intensity measurement and the uniformity was then calculated using Equation (8).

The angular response of concentrators was investigated by rotating the concentrator under a fixed light source as shown in Fig. 10. The VSC-PV assembly can be positioned on the rotary stage in one of the three possible directions as illustrated in Fig. 11: East-West (E-W), South-North (S–N), and Northwest-Southeast (NW-SE)/Southwest-Northeast (SW-NE). During the measurements, the VSC-PV assembly on the rotary stage was rotated at a step of 5° from 0° to ±45° and the I–V curves were obtained at each rotation. The concentration ratio as a function of AOI corresponding to each rotation were calculated.

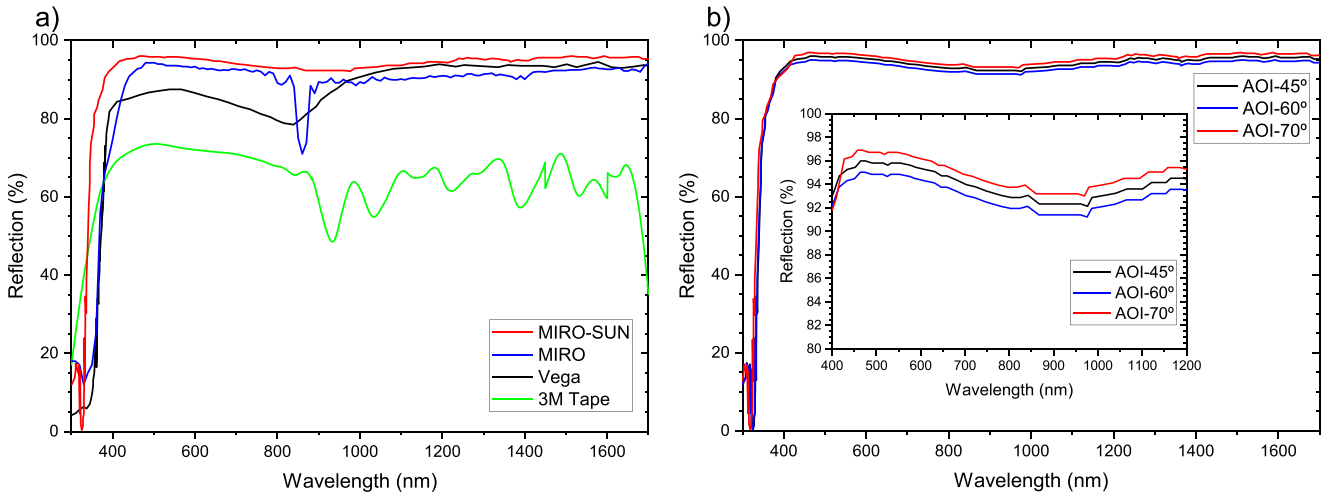

Fig. 6. The reflectance of reflectors (a) four different thin-film mirrors; and (b) the reflectance of the MIRO-SUN mirror at different AOIs.

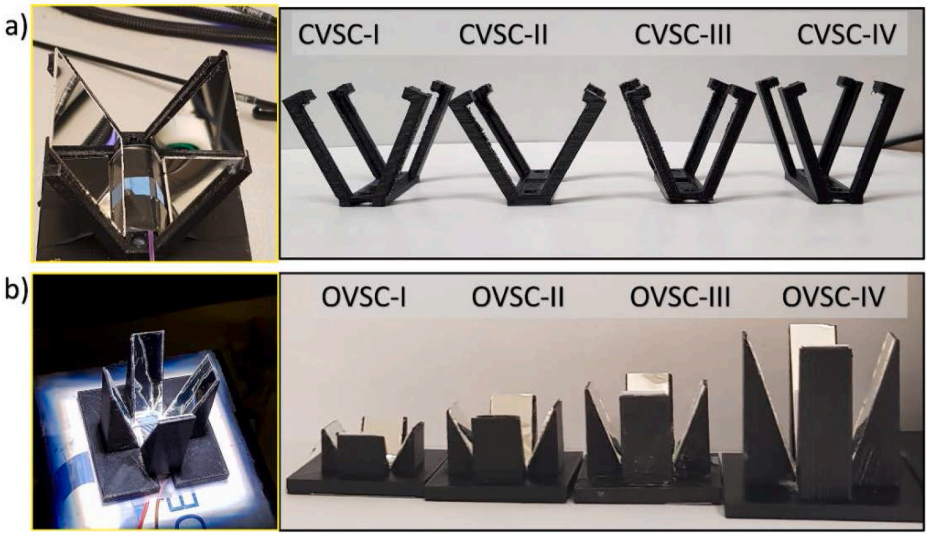

Fig. 7. A photograph for the fabricated VSCs (a) conventional VSCs (CVSCs); and (b) Onagraceae VSCs (OVSCs).

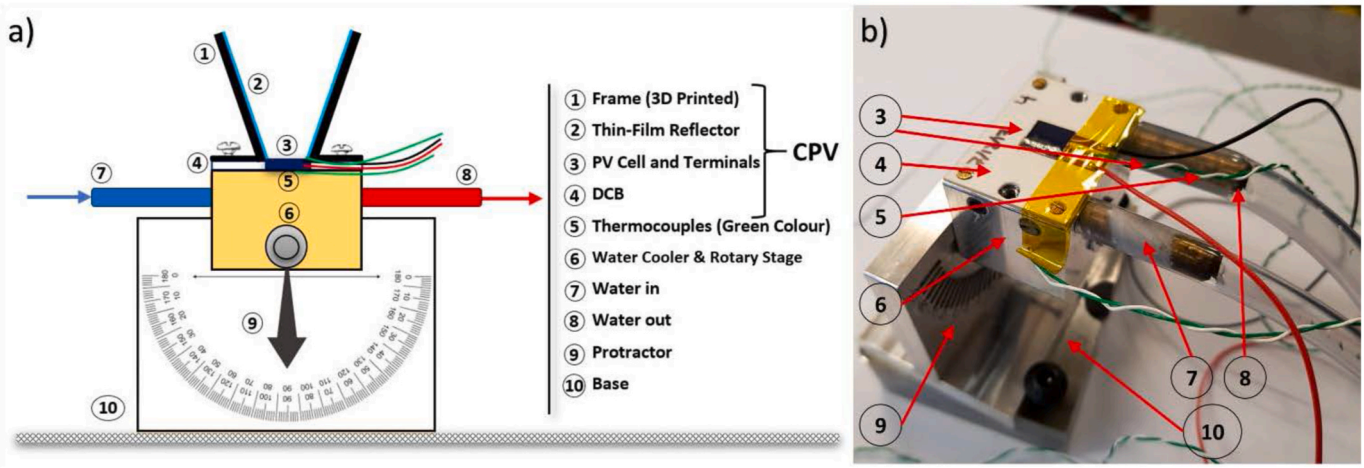

Fig. 8. VSC-PV assembly on a rotary stage for optical characterisation (a) schematic diagram of VSC-PV assembly and (b) photograph of the PV setup on rotary stage without concentrator.

4. Results and discussions

4.1. Optical and electrical performances

Fig. 12 shows the results of the concentration ratios for the CVSCs and OVSCs measured under normal incident irradiance. It can be seen that the actual concentration ratios for all concentrators are close to their corresponding theoretical values (i.e., the geometrical concentration ratio). Furthermore, the concentration ratio of OVSCs is approximately 1.5 times of their corresponding CVSCs of the same φ and aspect ratio (L/W_{ab}), demonstrating the advantage of the OVSCs for achieving the concentration ratio beyond the limit of conventional VSCs. More importantly, the concentration ratio of the OVSCs is increased without significant reduction in optical efficiency. It can be seen from Table 4 that the OVSCs have high optical efficiency (82%–92%), which is only slightly lower than that of the conventional VSCs but significantly higher than that of pyramid VSCs. The concentration ratio and optical efficiency were determined from measured I–V curves show good agreement with the values determined from the light intensity measurements by spectroradiometer. For both CVSCs and OVSCs, the optical efficiency increases with increasing concentration ratio. This can be attributed to increased tilt angle and reflector length of the concentrators, which minimise optical losses.

As a result of increased concentration, the power output of the OVSC-PV assembly is higher than that of the corresponding CVSC-PV assembly. Compared to the bare cell, the light intensity is increased by 4.72 times when using the concentrator OVSC-VI. This led to the increase in the power output by 5.21 times due to the improvement in I_{sc}, V_{oc} and FF. Consequently, the efficiency is increased from 12.6% of the bare cell to 14.0% using the concentrator OVSC-VI, confirming the well-known advantage of using concentrator system.

Fig. 13 presents the light uniformity across the absorber area of the fabricated concentrators. The results show that the uniformity is better than 95% for all concentrators except for the OVSC-VI. Although the uniformity of OVSCs appears to be slightly lower than the conventional VSCs, the advantage of good uniformity of the VSCs is essentially maintained in OVSCs because of the reduction is very small. The light uniformity seems to decrease slightly with increasing the concentration ratio and a noticeable reduction was observed in OVSC-VI. Nevertheless, its uniformity is still larger than 90%, which is significantly better than other types of concentrators such as CPC [53].

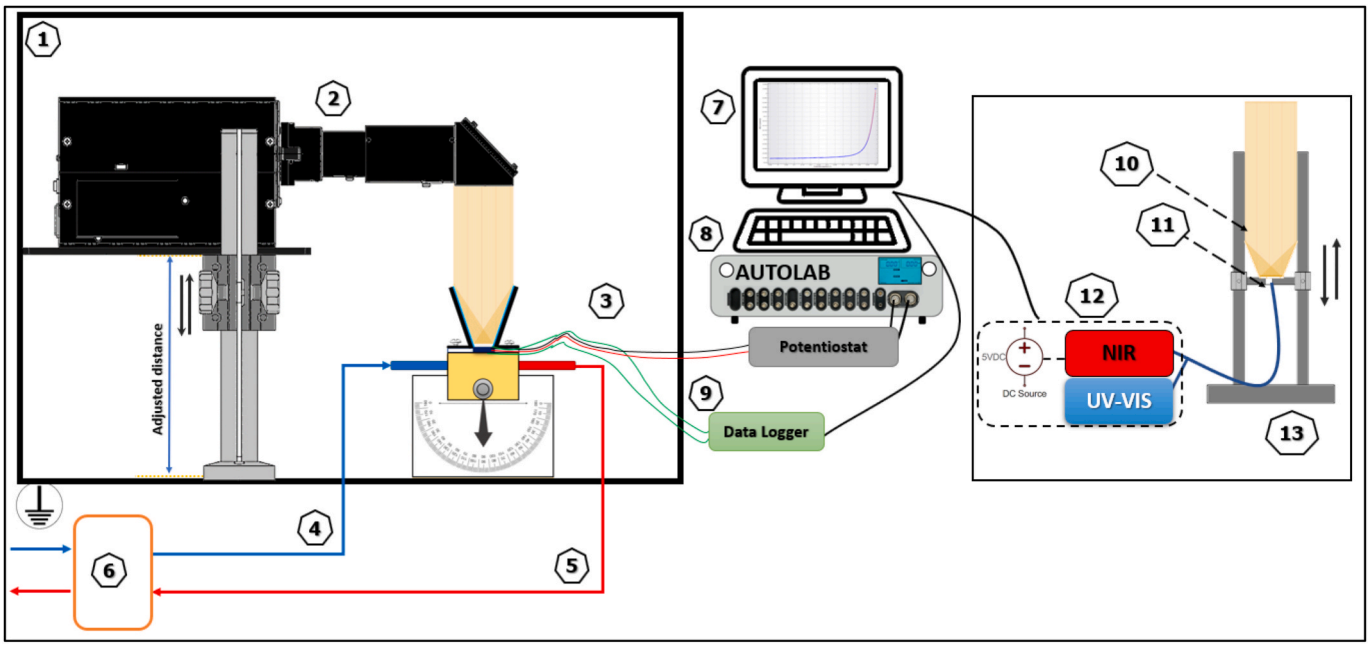

Fig. 9. Schematic diagram of the testing setup, consisting of (1) Faraday cage, (2) solar simulator, (3) the VSC-PV assembly, (4)the inlet of cooling water, (5) the outlet of cooling water, (6) temperature controlled water circulating bath, (7) PC; (8) AUTOLAB I–V tracer, (9) PICO-data logger, (10) VSC for spectral testing; (11) Spectral sensor, (12) Spectroradiometer, and (13) VSC holder for spectral testing.

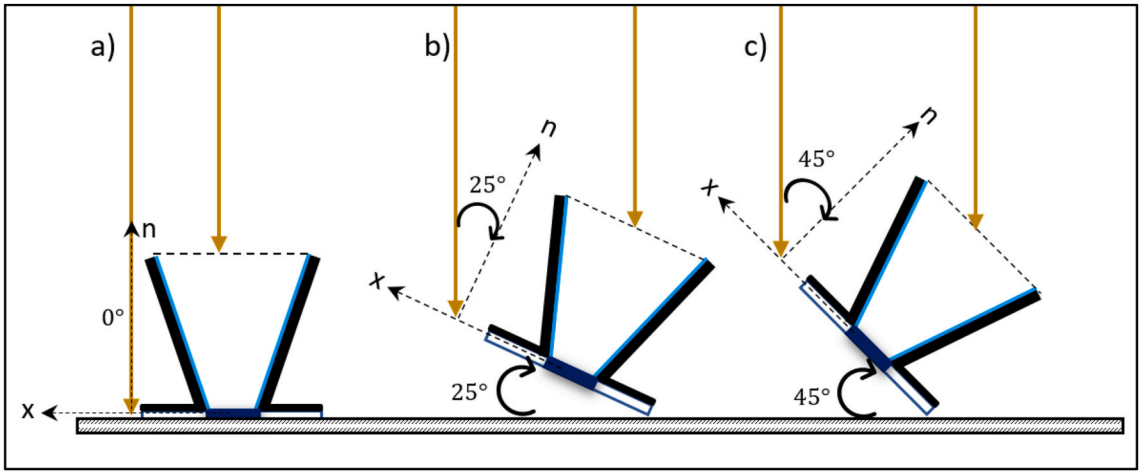

Fig. 10. The schematic diagram of the angular test of the VSC-PV assembly.

4.2. Angular response

Fig. 14 presents the experimental results of the angular responses for all fabricated concentrators. In general, the concentration ratio decreases with increasing the angle of light incidence (AOI) and it decreases more quickly for the concentrators with higher concentration ratio as shown Fig. 14a. In addition, the results show that the concentration ratio of the CVSCs decreases linearly with the AOI while the concentration ratio of the OVSCs decreases slowly initially but becomes increasingly fast with the AOI. This trend can be seen clearly in Figs. 14b and c for CVSCs and OVSCs, respectively, where the data are normalised to the maximum value of concentration ratio. The angular response of the bare Si cell is also included for comparison. It can be seen clearly that the reduction in the concentration ratio of the OVCSs is much smaller than that of the CVSCs within the initial 15°. This result demonstrates that the OVSCs have better angular response than the CVSCs of the same concentration ratio. It is to be noted that the data presented in Fig. 14 was obtained with the concentrators mounted on the rotary stage in the S–N direction. The tests were also carried out along the other directions. Although the data shows that the angular response is affected by the direction (Appendix), the trends and characteristics are very similar to those observed in the S–N directions. This is due to the symmetrical feature of the VSCs.

4.3. Reflector area and cost

This study focuses on the key concentrator components without considering the tracking system. Under this assumption, the reflector is a major cost in making the solar concentrators. It is therefore necessary to minimise the reflector area while maintaining the optical performance. Table 5 shows the design parameters for CVSC-IV and OVSC-I. Although both concentrators have the similar CR_{geo}, the total reflector area required to achieve this concentration ratio is 632 mm^2 for CVSC-IV and 400 mm^2 for OVSC-I. CVSC-IV consumes 58% more reflective material

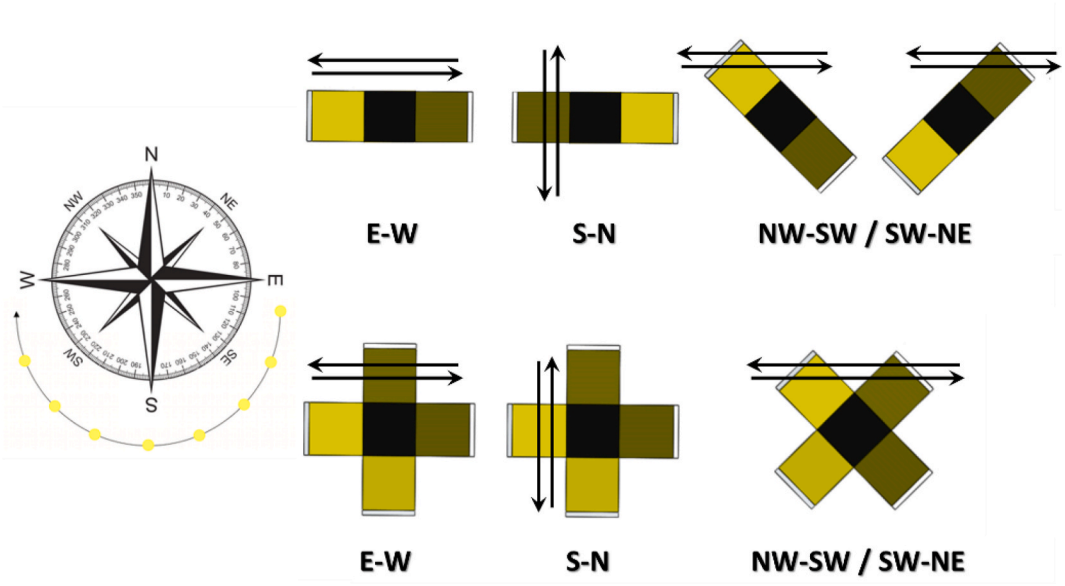

Fig. 11. Three possible rotation directions for angular response measurements of CVSCs and OVSCs.

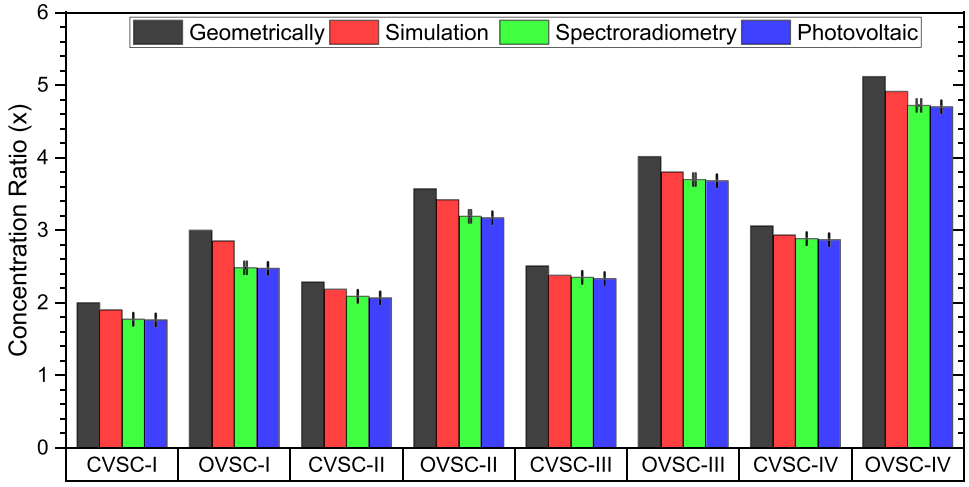

Fig. 12. The concentration ratios of the fabricated conventional VSCs and Onagraceae VSCs measured under normal irradiance of light.

Table 4
The electrical and optical performance of the VSC-PV assembly using conventional VSCs and OVSCs (V_{oc} is the open-circuit voltage, I_{sc} is the short-circuit current, FF is the fill factor, P_{max} is the maximum power output, η is the conversion efficiency, CR is the concentration ratio and OE is the optical efficiency).

φ	Mode	V_{oc} (Volt)	I_{sc} (mA)	FF (%)	P_{max} (mW)	η (%) ± 0.1%	CR (x) ± 0.01		OE (%) ± 0.01	
							PV	Spectro	PV	Spectro
–	Bare cell	0.585	26.98	75.86	11.98	12.6	-	-	-	-
60°	CVSC-I	0.600	47.59	77.24	22.05	13.2	1.76	1.77	88.2	88.6
	OVSC-I	0.610	66.75	77.67	31.62	13.5	2.47	2.48	82.5	82.7
65°	CVSC-II	0.605	55.78	77.43	26.12	13.3	2.07	2.09	90.4	91.4
	OVSC-II	0.615	85.58	77.76	40.92	13.6	3.17	3.19	88.8	89.4
68°	CVSC-III	0.607	62.97	77.59	29.65	13.4	2.33	2.35	93.0	93.7
	OVSC-III	0.623	99.34	78.06	48.31	13.8	3.68	3.70	91.7	92.1
71°	CVSC-IV	0.610	77.44	78.08	36.88	13.5	2.87	2.89	93.8	94.3
	OVSC-IV	0.629	126.86	78.19	62.39	14.0	4.70	4.72	91.8	92.2

than OVSC-I. Experimentally, the actual concentration ratio is 2.87x for the CVSC-IV and 2.47x for OVSC-I. This may be attributed to more optical losses in OVSCs. Nevertheless, it can be seen that even OVSC-II (Table 4), which has an actual concentration ratio of 3.17x, uses 4% less of the reflector material than CVSC-IV, demonstrating clearly the economic benefit of OVSCs.

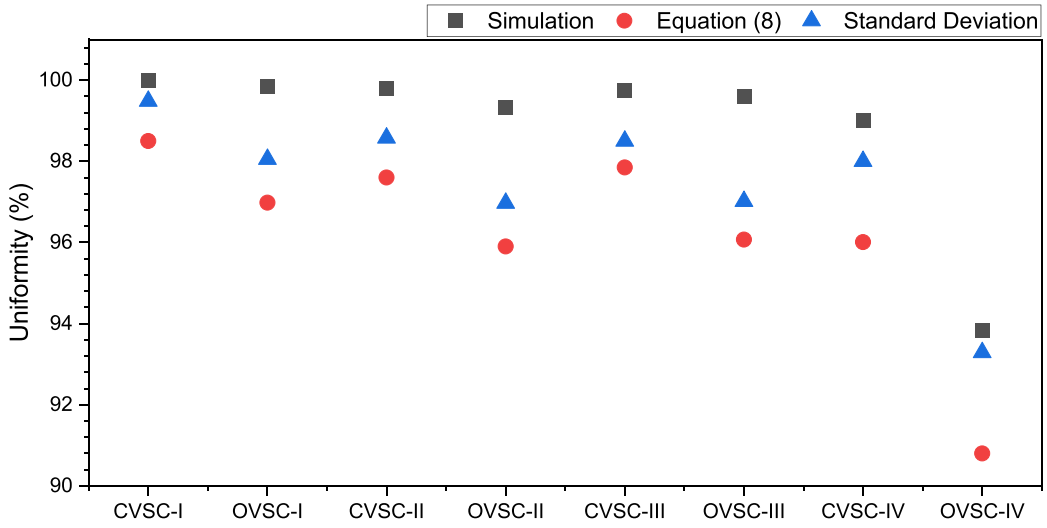

Fig. 13. The light uniformity of the conventional VSCs and Onagraceae VSCs.

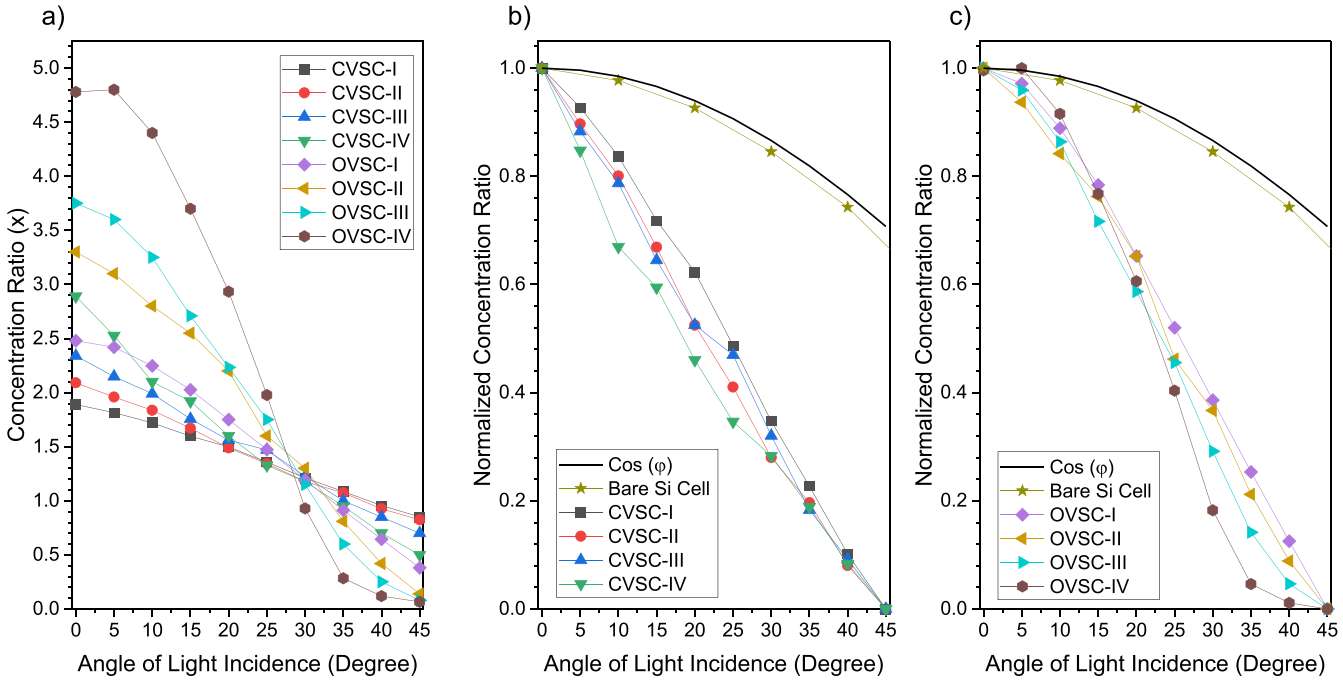

Fig. 14. The angular response of CVSCs and OVSCs a) concentration ratio as a function of AOI, b) the normalised concentration ratio as a function of AOI for CVSCs, and c) the normalised concentration ratio as a function of AOI for OVSCs. Standard deviation between the repeated measurements is less than 1%. The data was obtained with the concentrators mounted on the rotary stage in the S–N direction.

Table 5
Design parameters of the CVSC-IV and OVSC-I.

Parameter	CVSC-IV	OVSC-I
Aperture area (mm^2)	306	300
Area of reflectors (mm^2)	632	400
VSC height (mm)	29.91	8.66
Reflector tilt angle, φ	70°	60°
Aspect ratio, (L/ W_{ab})	3.16	1.00
Concentration ratio, CR_{geo}	3.06x	3.00x

Table 6 shows the estimated cost for three conceptual CPV systems compared to a commercial flat PV panel (SolarWatt, 320W_p, [55]). The CPV systems using CVSC-IV, OVSC-I and OVSC-IV, respectively, were arranged to achieve the same nominal power (320 W) of the flat PV panel that consists of 60 Si cells. The cost estimation considered the cost of the PV cells, materials for making the concentrator frames, aluminium reflectors, and electrical wires. The CPV systems using CVSC-IV and OVSC-IV have the same reflector tilt angle φ, whereas the systems using CVSC-IV and OVSC-I have the same geometrical concentration ratio, CR_{geo}. The use of the concentrators CVSC-IV, OVSC-I and OVSC-IV can save about 65%, 65% and 80% of the PV cells, respectively. However, only the system using OVSC-I is able to reduce the cost slightly below the cost of the flat panel system. It is to be noted that the comparison shown in Table 6 is a simplistic case to illustrate the advantages of the new design based on the costs involved in this project without considering other factors. Particularly, the costs are calculated based on an ideal case

Table 6
The estimated cost of conceptual CPV systems producing a nominal power of 290 W (The calculation is based on an ideal case where the sunlight is perpendicular to the solar cell surface. The angular response of the systems has not been considered).

	Flat Panel [55]	OVSC-IV	CVSC-IV	OVSC-I
PV cell area	156 mm × 156 mm 156 mm × 156 mm 156 mm × 156 mm 156 mm × 156 mm			
No. of PV cells	60	12	21	21
Total area of PV cells	1.46 m^2	0.30 m^2	0.51 m^2	0.51 m^2
No. of concentrators	No concentration	12	21	21
Aperture area/ height	1.66 m^2/0.04 m	1.50 m^2/ 0.5 m	1.57m^2/ 0.5 m	1.54m^2/ 0.16 m
Reflector area (m^2)	–	3.70	3.23	2.04
Cost of PV cells ($) [55]	–	29.87	52.27	52.27
Cost of reflectors ($) [56]	–	205.11	179.48	116.93
Structure ($) [57]	–	119.09	104.21	75.86
Total Cost	**$288.90**	**$354**	**$336**	**$245**

(i) The cost of the PV cell is $2.49, (ii) the cost of reflector is $56/$m^2$, (iii) the structure cost is estimated from the printer's CURA software ($0.01/$cm^3$) material and power, and (iv) the total costs include the VAT (20%).

where the sunlight is perpendicular to the solar cell surface. In practice, daily energy production of a photovoltaic system is depended on angular response of the system. In general, the angular response of a concentrator system is poor compared to a flat panel system. Consequently, the estimated costs for the concentrator systems shown in Table 6 are likely to be higher than the flat panel system due to additional cost for a tracking system or due to less daily energy production without a tracking system. Clearly, it is extremely challenging for CPV systems to compete with the flat silicon PV systems due to very competitive price of silicon solar cells. Nevertheless, such concentrators may find applications in CPV systems that employ other types of more expensive solar cells, such as GaAs and InP cells.

5. Conclusions

A new configuration of V-trough solar concentrator, referred to as the Onagraceae V-trough Solar Concentrator (OVSC), was investigated in comparison with conventional V-trough concentrators. Four OVSCs of different concentration ratios, together with four corresponding conventional VSCs, were fabricated and their optical performances were characterised. The experimental results from this comparative study show that this new configuration enables to achieve higher concentration ratio beyond the limits of the conventional V-trough concentrators of the same tilt angle and reflector length. The higher concentration ratio is achieved without significant reduction in optical efficiency (less than 2% on average) and light uniformity (~1% on average), which is a challenging trade-off in the design of solar concentrators. Furthermore, the additional advantages of this new configuration include the improved angular response and potential to reduce the cost of the concentrators by using less reflector area for the same concentration ratio compared to the conventional V-trough concentrators. Clearly, these characteristics make OVSC a better alternative for low cost and low concentration applications. In addition, the flat surface of the reflector area facilitates direct implementation of this configuration for fabricating spectral splitting concentrator using commercially available dichroic mirrors. It is worth noting that the potential application and economic benefit of this novel design is still unclear. Considering the recent dramatic reduction in the price of silicon solar cells, the use of the concentrators to improve the economic performance of silicon solar cells is no longer considered a viable route. Nevertheless, it is still possible to use the concentrators to improve the economic viability of other types of solar cells, such as GaAs or InP cells. In addition, the concentrators could also be employed to produce concentrated heat for varies thermal devices.

Appendix

CRediT authorship contribution statement

Mohammad Alnajideen: Writing – review & editing, Writing – original draft, Visualization, Validation, Methodology, Investigation, Formal analysis, Data curation, Conceptualization. **Min Gao:** Writing – review & editing, Validation, Supervision, Resources, Project administration, Funding acquisition, Conceptualization.

Declaration of competing interest

The authors declare that they have no known competing financial interests or personal relationships that could have appeared to influence the work reported in this paper.

Data availability

Information on the data underpinning the results presented here, including how to access them, can be found in the Cardiff University data catalogue at [10.17035/d.2022.0200702353].

Acknowledgement

One of the authors (M.A) would like to acknowledge the financial support by Mutah University, the Hashemite Kingdom of Jordan. Dr Pedro Bonilla Villalba for his help in MATLAB and Dr Mazin Al-Shidhani for using the rotary stage. We would like to thank ALANOD GmbH & Co. KG for supplying the aluminium sheet reflectors used in this work. The authors would like to thank the Mechanical and Electrical Workshops at Cardiff School of Engineering for their assistance in constructing the required setups for this research. The facilities for solar cell characterisation were established with the funding support by EPSRC under the projects EP/K029142/1, EPK022156/1.

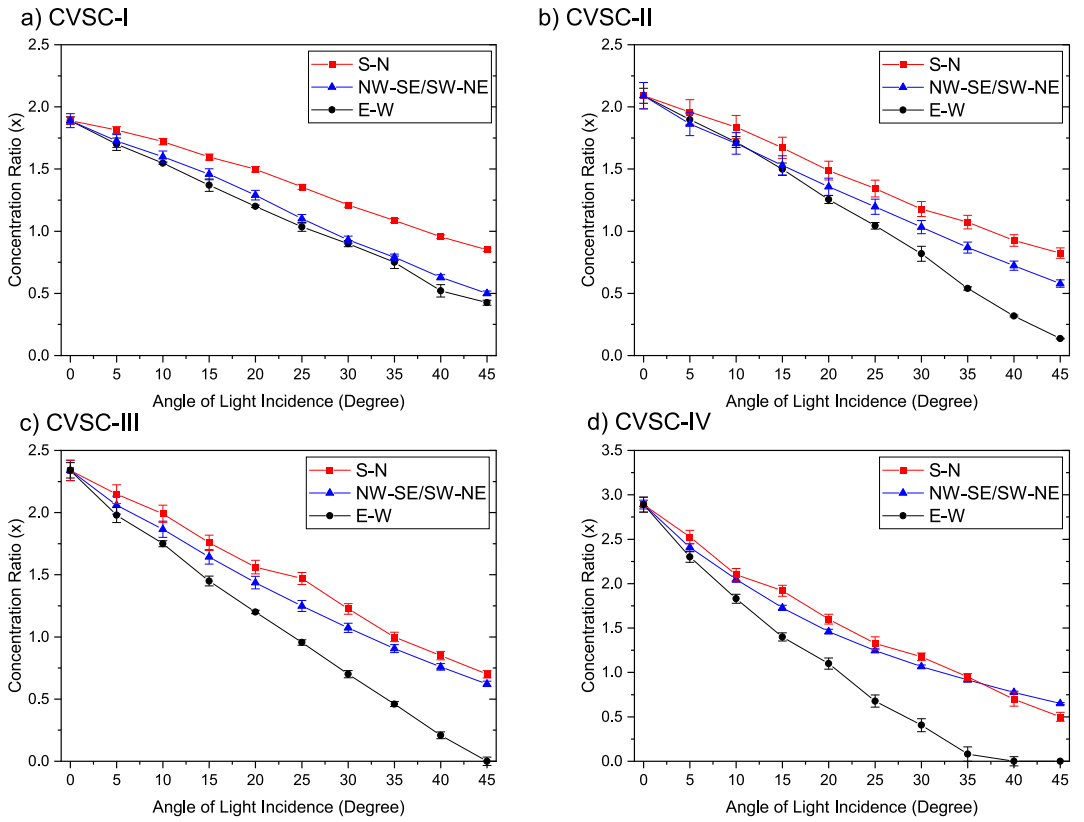

Fig. A- 1. The angular response of Conventional VSCs.

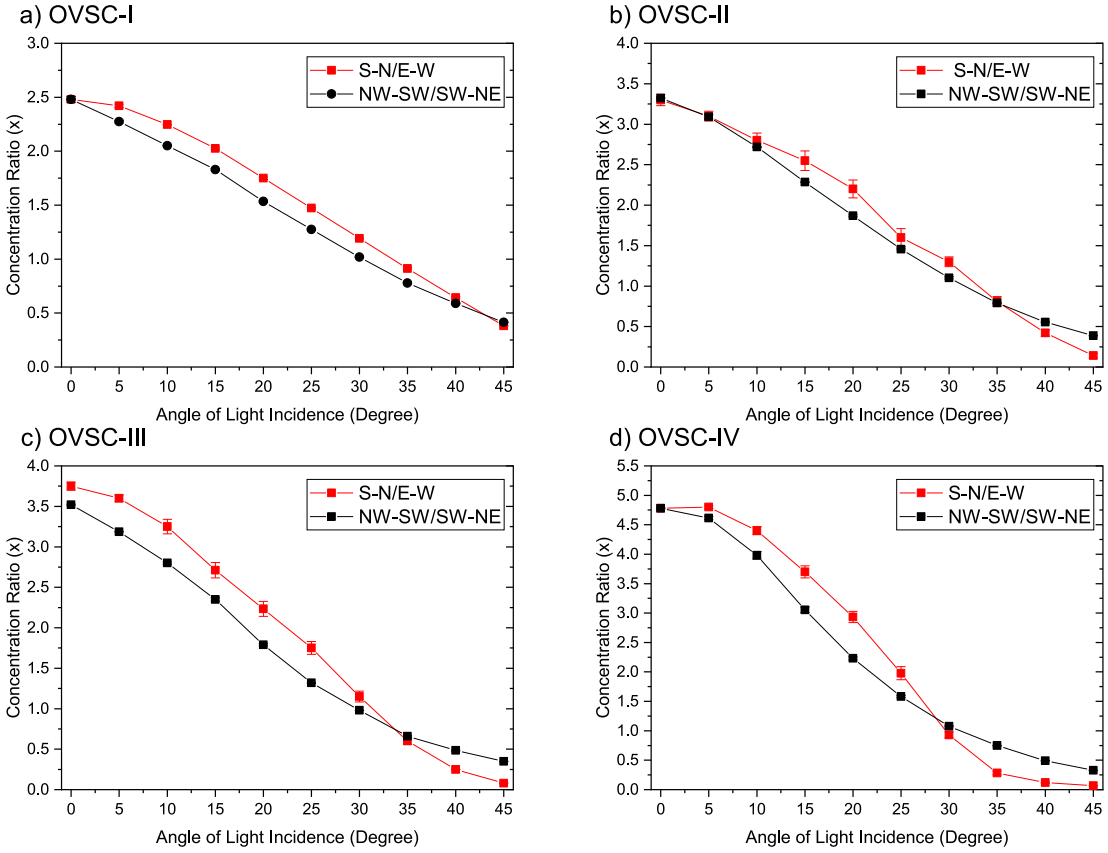

Fig. A- 2. The angular response of Onagraceae VSCs.

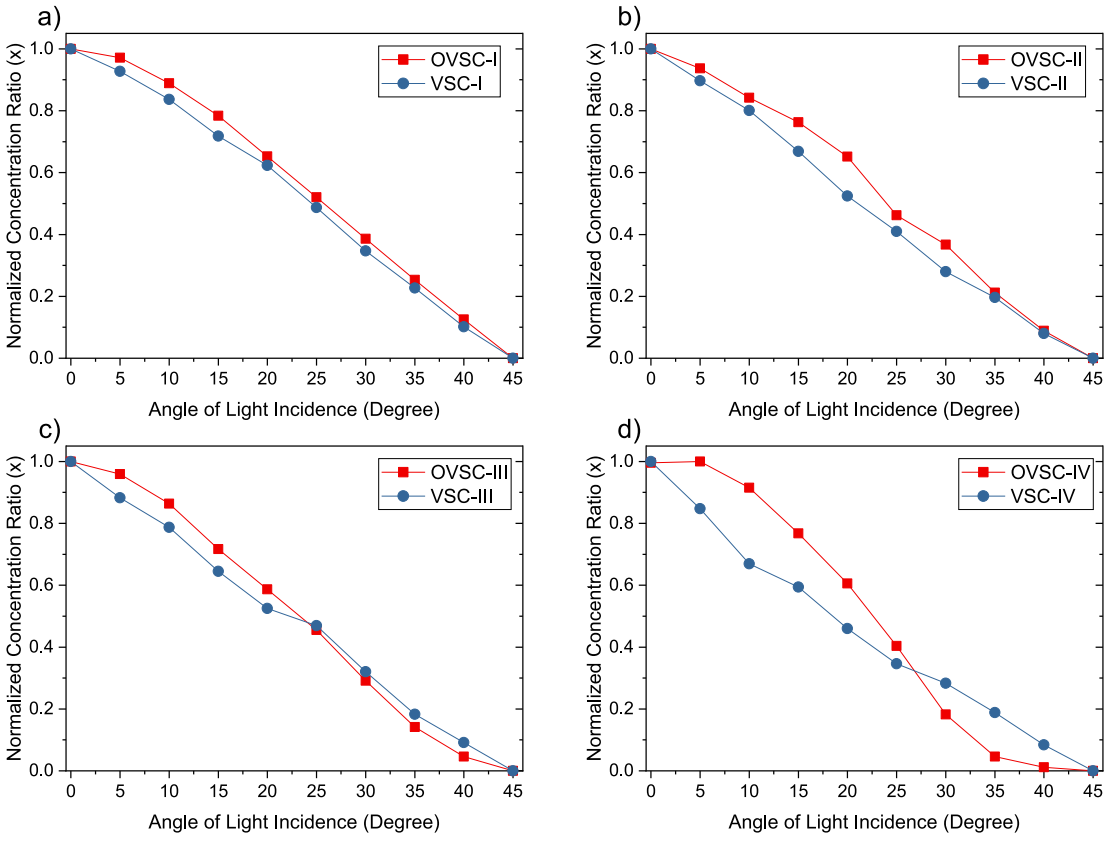

Fig. A- 3. Comparison of the angular response between the CVSCs and OVSCs in the S–N position.

References

[1] R. Winston, Principles of solar concentrators of a novel design, Sol. Energy 16 (2) (1974) 89–95.
[2] S.A. Omer, D.G. Infield, Design and thermal analysis of a two stage solar concentrator for combined heat and thermoelectric power generation, Energy Convers. Manag. 41 (7) (2000) 737–756.
[3] G.O. Prado, L.G.M. Vieira, J.J.R. Damasceno, Solar dish concentrator for desalting water, Sol. Energy 136 (2016) 659–667.
[4] P. Yeh, N. Yeh, Design and analysis of solar-tracking 2D Fresnel lens-based two staged, spectrum-splitting solar concentrators, Renew. Energy 120 (2018) 1–13.
[5] T. Osório, et al., One-Sun CPC-type solar collectors with evacuated tubular receivers, Renew. Energy 134 (2019) 247–257.
[6] A. Dang, Detailed optical and thermal analysis of trough-like concentrators using tubular absorbers, Energy Convers. Manag. 25 (2) (1985) 147–158.
[7] P.D. Jones, L. Wang, Concentration distributions in cylindrical receiver/paraboloidal dish concentrator systems, Sol. Energy 54 (2) (1995) 115–123.
[8] R.P. Goswami, et al., Optical designs and concentration characteristics of a linear Fresnel reflector solar concentrator with a triangular absorber, Sol. Energy Mater. 21 (2–3) (1990) 237–251.
[9] X. Liu, R. Tang, Design optimization of fixed V-trough concentrators, in: Asia-Pacific Power and Energy Engineering Conference, APPEEC, 2010.
[10] O.Z. Sharaf, M.F. Orhann, Concentrated photovoltaic thermal (CPVT) solar collector systems: Part II - implemented systems, performance assessment, and future directions, Renew. Sustain. Energy Rev. 50 (2015) 1566–1633.
[11] H. Boumaaraf, et al., Experimental study of low-concentrator photovoltaic systems: electrical and thermal, Electr. Eng. 100 (4) (2018) 2569–2578.
[12] K.K. Chong, et al., Design and development in optics of concentrator photovoltaic system, Renew. Sustain. Energy Rev. 19 (2013) 598–612.
[13] J. Aguilera, Introduction, in: P. Pérez-Higueras, E.F. Fernández (Eds.), High Concentrator Photovoltaics: Fundamentals, Engineering and Power Plants, Springer International Publishing, Cham, 2015, pp. 1–8.
[14] H. Apostoleris, M. Stefancich, M. Chiesa, Tracking-integrated systems for concentrating photovoltaics, Nat. Energy 1 (2016), 16018.
[15] J. Freilich, J.M. Gordon, Case study of a central-station grid-intertie photovoltaic system with V-trough concentration, Sol. Energy 46 (5) (1991) 267–273.
[16] D. Freier, et al., A review of optical concentrators for portable solar photovoltaic systems for developing countries, Renew. Sustain. Energy Rev. 90 (2018) 957–968.
[17] S. Madala, R.F. Boehm, A review of nonimaging solar concentrators for stationary and passive tracking applications, Renew. Sustain. Energy Rev. 71 (2017) 309–322.
[18] D. Chemisana, Building integrated concentrating photovoltaics: a review, Renew. Sustain. Energy Rev. 15 (1) (2011) 603–611.
[19] B. Norton, et al., Enhancing the performance of building integrated photovoltaics, Sol. Energy 85 (8) (2011) 1629–1664.
[20] F. Muhammad-Sukki, et al., Mirror symmetrical dielectric totally internally reflecting concentrator for building integrated photovoltaic systems, Appl. Energy 113 (2014) 32–40.
[21] N. Sellami, T.K. Mallick, D.A. McNeil, Optical characterisation of 3-D static solar concentrator, Energy Convers. Manag. 64 (2012) 579–586.
[22] H. Baig, et al., Outdoor performance of a reflective type 3D LCPV system under different climatic conditions, in: 13th International Conference on Concentrator Photovoltaic Systems, vol. 2017, American Institute of Physics Inc, 2017. CPV.
[23] H. Baig, et al., Indoor characterization of a reflective type 3D LCPV system, in: 12th International Conference on Concentrator Photovoltaic Systems, vol. 2016, American Institute of Physics Inc, 2016. CPV.
[24] S.H. Abu-Bakar, et al., Optimisation of the performance of a novel rotationally asymmetrical optical concentrator design for building integrated photovoltaic system, Energy 90 (1) (2015) 1033–1045.
[25] F. Yang, et al., Design and experimental study of a cost-effective low concentrating photovoltaic/thermal system, Sol. Energy 160 (2018) 289–296.
[26] H. Chen, et al., Experimental investigation of a novel LCPV/T system with micro-channel heat pipe array, Renew. Energy 115 (2018) 773–782.
[27] H.W. Liu, H. Zhang, H.P. Chen, Performance analysis of a novel LCPV/T system, IOP Conf. Ser. Earth Environ. Sci. 188 (2018), 012067.
[28] M. Al-Shidhani, Design, Fabrication and Characterisation of Cross Compound Parabolic Concentrators for Solar Power Generation, Cardiff University, 2020.
[29] R. Künnemeyer, et al., Performance of a V-trough photovoltaic/thermal concentrator, Sol. Energy 101 (2014) 19–27.
[30] G. Li, J. Tang, R. Tang, Performance and design optimization of a one-axis multiple positions sun-tracked V-trough for photovoltaic applications, Energies 12 (6) (2019).
[31] H.F. Chiam, Bi-yearly adjusted V-trough concentrators, Sol. Energy 28 (5) (1982) 407–412.
[32] M.I. Irshid, M.O. Othman, V-troughs with high concentration ratios for photovoltaic concentrator cells, Sol. Cell. 23 (3–4) (1988) 159–172.
[33] Y. Wang, et al., Photovoltaic and disinfection performance study of a hybrid photovoltaic-solar water disinfection system, Energy 106 (2016) 757–764.

[34] Z. Su, et al., Analysis of a photovoltaic-electrolyser direct-coupling system with a V-trough concentrator, Energy Convers. Manag. 108 (2016) 400–410.
[35] H. Singh, M. Sabry, D.A.G. Redpath, Experimental investigations into low concentrating line axis solar concentrators for CPV applications, Sol. Energy 136 (2016) 421–427.
[36] K.G.T. Hollands, A concentrator for thin-film solar cells, Sol. Energy 13 (2) (1971) 149–163.
[37] M.I.A. Hadi, Analysis and performance of a V-trough solar concentrator, Can. J. Chem. Eng. 63 (3) (1985) 399–405.
[38] N. Fraidenraich, G.J. Almeida, Optical properties of V-trough concentrators, Sol. Energy 47 (3) (1991) 147–155.
[39] M.M. Sorour, R.A. Mahmoud, Design of stationary finite length V-trough Solar collector, Int. J. Sol. Energy 10 (1–2) (1991) 63–81.
[40] N. Fraidenraich, Analytic solutions for the optical properties of v-trough concentrators, Appl. Opt. 31 (1) (1992) 131–139.
[41] N. Fraidenraich, Analytic solutions for the optical and radiative properties of nonaccepted light radiation of V-trough concentrators, Appl. Opt. 34 (22) (1995) 4800–4811.
[42] N. Fraidenraich, Design procedure of V-trough cavities for photovoltaic systems, Prog. Photovoltaics Res. Appl. 6 (1) (1998) 43–54.
[43] M. Alonso Abella, et al., Operation of standard PV modules in V-trough concentrators, in: Conference Record of the IEEE Photovoltaic Specialists Conference, 2005.
[44] N. Martín, J.M. Ruiz, Optical performance analysis of V-trough PV concentrators, Prog. Photovoltaics Res. Appl. 16 (4) (2008) 339–348.
[45] R. Tang, X. Liu, Optical performance and design optimization of V-trough concentrators for photovoltaic applications, Sol. Energy 85 (9) (2011) 2154–2166.
[46] J. Bione, O.C. Vilela, N. Fraidenraich, Comparison of the performance of PV water pumping systems driven by fixed, tracking and V-trough generators, Sol. Energy 76 (6) (2004) 703–711.
[47] C.S. Solanki, et al., Enhanced heat dissipation of V-trough PV modules for better performance, Sol. Energy Mater. Sol. Cell. 92 (12) (2008) 1634–1638.
[48] G.M. Tina, P.F. Scandura, Case study of a grid connected with a battery photovoltaic system: V-trough concentration vs. single-axis tracking, Energy Convers. Manag. 64 (2012) 569–578.
[49] V.N. Palaskar, S.P. Deshmukh, A.B. Pandit, Design and performance analysis of reflectors attached to commercial PV module, Int. J. Renew. Energy Resour. 4 (1) (2014) 240–245.
[50] L. Qin, et al., Comparison of photovoltaic and photocatalytic performance of non-concentrating and V-trough SOLWAT (solar water purification and renewable electricity generation) systems for water purification, Energy 85 (2015) 251–260.
[51] K. Narasimman, I. Selvarasan, Design construction and analysis of solar ridge concentrator photovoltaic (PV) system to improve battery charging performance, Ecotoxicol. Environ. Saf. 127 (2016) 187–192.
[52] M. Al-Najideen, M. Al-Shidhani, G. Min, Optimum design of V-trough solar concentrator for photovoltaic applications, in: AIP Conference Proceedings., AIP Publishing LLC, 2019.
[53] M. Al-Shidhani, et al., Design and testing of 3D printed cross compound parabolic concentrators for LCPV system, in: 14th International Conference on Concentrator Photovoltaic Systems, vol. 2018, American Institute of Physics Inc, 2018. CPV.
[54] ASTM, Standard Specification for Solar Simulation for Photovoltaic Testing, ASTM International, 2015.
[55] SolarWatt, SOLARWAT T 60M High Power, 2019.
[56] Alanod-Solar, MIRO-SUN® Reflective, vol. 95, ALANOD GmbH & Co. KG, Germany, 2017.
[57] Ultimaker 2 Extended + 3D Printer 9626, (USA).